Sensors & Transducers Journal, Vol. 137, Issue 2, February 2012, pp. 104-114

www.sensorsportal.com

Sensors & Transducers

ISSN 1726-5479

http://www.sensorsportal.com

Room Temperature Liquefied Petroleum Gas Sensing Polymer (n-polypyrrole/p-polyaniline) Based Heterojunction

S. V. Patil, P. R. Deshmukh, * C. D. Lokhande
Thin Film Physics Laboratory, Department of Physics, Shivaji University,
Kolhapur - 416004 (M.S), India
* Tel.: +91 231 2609225, fax: +91 231 2692333
E-mail: l_chandrakant@yahoo.com (Prof. C. D. Lokhande)

Received: 4 December 2011 /Accepted: 14 February 2012 /Published: 28 February 2012

Abstract: In the present work, room temperature (300 K) liquefied petroleum gas (LPG) sensor based on n-polypyrrole/p-polyaniline (n-PPy/p-PANI) heterojunction has been fabricated using simple inexpensive electrodeposition method. The n-PPy/p-PANI heterojunction was fabricated by depositing polyaniline over predeposited polypyrrole thin film. The polypyrrole and polyaniline thin films were characterized for their structural and surface morphological properties and chemical properties. The Raman spectrum of polyaniline and polypyrrole thin films confirmed the formation of polyaniline and polypyrrole. The X-ray diffraction (XRD) studies revealed that polypyrrole and polyaniline films are amorphous. The n-PPy/p-PANI heterojunction showed selectivity towards LPG as compared to N_2 and CO_2. The room temperature maximum gas response of 33 % (± 3 %) was achieved upon exposure of LPG at 1040 ppm. *Copyright © 2012 IFSA.*

Keywords: Thin films, Chemical sensor, Polyaniline/polypyrrole, Heterojunction, LPG sensor.

---

1. Introduction

Gases are vital in many industrial and domestic activities. In the last decade, a specific demand for gas detection and monitoring has emerged particularly as the leakage of gases may cause plenty of serious problems. Many commercial gas sensors are available which operates on different gas sensing principles. Among these widely adopted are the semiconductor metal oxide gas sensor devices which have several unique advantages such as low cost, small size, measurement simplicity, durability, ease of fabrication, and low detection limits (< ppm levels)[1]. However, they have disadvantages such as low selectivity to specific gases and lower sensitivity [2-3]. Further, all metal oxide sensors operate at high temperature and principle of operation is based on the change in conductivity or resistance of material by interaction with gas molecules [4-5].

A recent focus is on conducting polymers like polyaniline, polypyrrole and other conducting polymers due to their attractive features such as ease of preparation, high stability and high conductivity. Among conducting polymers, polyaniline and polypyrrole have been widely studied in the development of gas sensors due to their physical properties, enhanced gas response and room temperature operation [6]. Arsat et al [7] used polyaniline nanofibers for sensing hydrogen gas at room temperature. Ayad et al [8] developed phosphoric acid and pH sensors based on polyaniline thin films. Ammonia gas sensor has been developed by Hernandez et al [9] using polypyrrole nanowires at room temperature. Yang et al [10] used polypyrrole nanofibers for NH_3 gas at room temperature.

In order to abolish the temperature requirement and other problems of metal oxide semiconductors, many research groups have been developing gas sensor technology based on inorganic-organic or inorganic-inorganic heterojunctions, which show sensitivity to different gases at room temperature. Dhawale et al [11] fabricated n-CdS/p-polyaniline heterojunction as a LPG sensor at room temperature with 80 % gas response. Herrán et al [12] reported $BaTiO_3$–CuO thin film heterojunction which detects carbon dioxide at room temperature. Ladhe et al [13] fabricated complete inorganic room temperature n-Bi_2S_3-p-CuSCN heterojunction which showed 70 % response towards LPG, room temperature LPG sensor based on p-polyaniline/n-TiO_2 heterojunction with 63 % gas response has been fabricated by Dhawale et al [14]. Joshi et al [15] developed n-CdTe/p-polyaniline heterojunction based room temperature LPG sensor with 70% gas response. Dhawale et al [16] fabricated p-polyaniline/n-ZnO thin film heterojunction sensor for room temperature LPG detection and exhibited 81% gas response towards LPG. A room temperature LPG sensor based on n-CdSe/p-polyaniline junction has been fabricated by Joshi et al [17] which showed gas response of 67.7 %.

In this work, we have fabricated organic-organic (p-polyaniline/n-polypyrrole) based heterojunction using simple inexpensive electrodeposition method which showed gas sensing properties at room temperature. The polypyrrole and polyaniline thin films were deposited using galvanostatic mode. These films were characterized by X-ray diffraction pattern (XRD), scanning electron microscopy (SEM) and Raman spectroscopy techniques. The gas sensing properties of the heterojunction were studied at different concentrations ranging from 260 to 1300 ppm at room temperature. The results showed that n-PPy/p-PANI heterojunction exhibits good sensitivity, fast response and good recovery.

2. Experimental

2.1. Deposition of Polypyrrole Thin Films

The conventional three electrode cell consisting graphite plate as a counter electrode, saturated calomel electrode (SCE) as a reference electrode and stainless steel substrate as a working electrode was used for the deposition of polypyrrole. Polypyrrole thin films were galvanostatically electrodeposited on stainless steel (SS) substrate from an aqueous bath containing 0.03 M pyrrole + 0.1 M KNO_3. The solution was prepared in freshly prepared double distilled water. The galvanostatic deposition of well adherent and uniform black colored polypyrrole thin film was obtained after passing a current 5 mA/cm^{-2} for 300 s. The polymerisation of pyrrole is commenced by the oxidation of pyrrole monomers to form pyrrole radicals. Two of these radicals then react to form a dimer as shown Fig. 1. As oxidizing potential of dimer is less than monomer, the dimers may be oxidised and larger oligomers can be formed. Subsequent further reactions (radicalisation and coupling) can take place between the oligomers formed, as long as electric current is supplied [18].

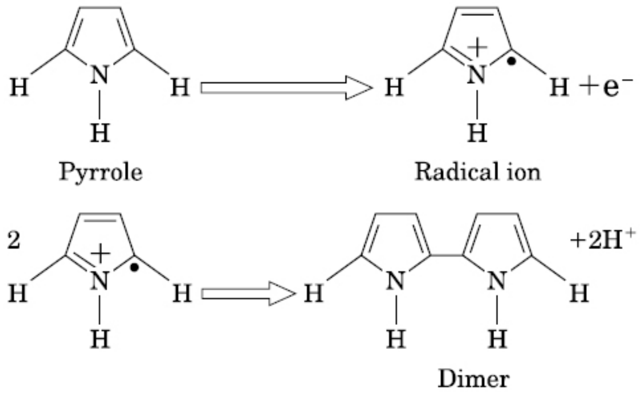

Fig. 1. Polymerization mechanism of pyrrole.

2.2. Deposition of Polyaniline Thin Films

For the fabrication of n-PPy/p-PANI heterojunction, the polyaniline was electrodeposited on predeposited polypyrrole thin film at room temperature from an aqueous solution containing 0.45 M aniline ($C_6H_5NH_2$) + 0.5 M H_2SO_4. The solution was prepared in freshly prepared double distilled water. Polyaniline was deposited on predeposited polypyrrole thin films by galvanostatic mode passing current of 4 mA/cm^{-2} for 300 s. The polymerization of polyaniline is commenced by the oxidation of pyrrole monomers as shown in Fig. 2. Radical coupling and elimination of two protons make mainly paraformed dimers. Chain propagation proceeds with oxidation of the dimer and aniline monomer on the electrode surface.

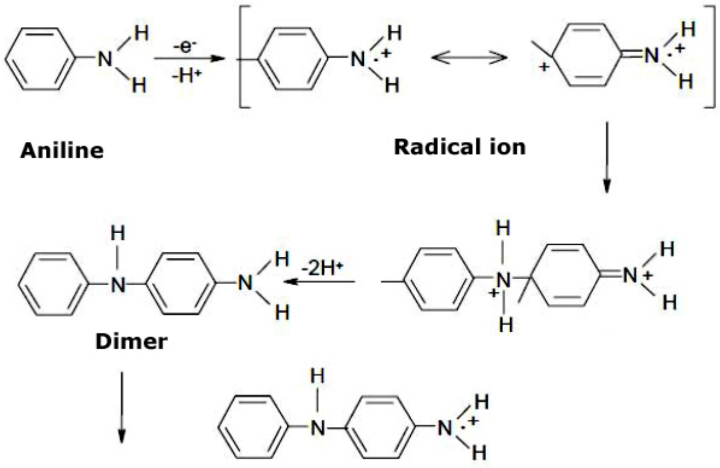

Fig. 2. Polymerization mechanism of aniline.

2.3. Fabrication of n-PPy/p-PANI Heterojunction

The schematic diagram and actual photograph of the n-PPy/p-PANI heterojunction is illustrated in Fig. 3 (a) and (b). It consists of a stainless steel substrate, onto which polypyrrole and polyaniline films are deposited subsequently by electrodeposition method. Top and back contacts are drawn with the help of silver paste. The diameter of contacts was around 0.1 cm.

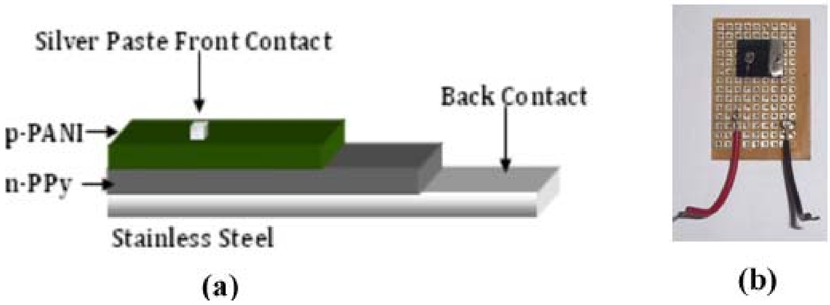

(a) (b)

Fig. 3. (a) Schematic diagram, and (b) actual photograph of the n-PPy/p-PANI heterojunction.

The forward biased I–V characteristics of the junction before and after exposure to different gases were recorded at different concentrations in the range of 260 to 1300 ppm in a voltage range of 0 to + 1.6 V. From the plot, maximum current change was recorded at a fixed voltage (+ 1.6 V). The electrical currents of n-PPy/p-PANI heterojunction in air (Ia) and in the presence of gas (Ig) were measured and using the following relation, the gas response was calculated.

$$S(\%) = \frac{I_a - I_g}{I_a} \times 100 = \frac{\Delta I}{I_a} \times 100 \quad (1)$$

2.4. Construction of Band Diagram of n-PPy/p-PANI Heterojunction

Fig. 4 shows energy band diagrams of n-PPy/p-PANI heterojunction before (a) and after (b) contact. To construct a band diagram, equilibrium chemical potentials of polypyrrole and polyaniline were separately measured in 1 M KCl solution with respect to saturated calomel electrode. Then measured equilibrium chemical potentials were converted into electrochemical scale to fix the Fermi level of polypyrrole and polyaniline. It is assumed that Fermi level lies at 0.05 eV below from conduction band of n-polypyrrole and above valence band for p-polyaniline [19]. The value of work function (Φ_1) of polyaniline is 4.85 eV and the value of work function (Φ_2) of polypyrrole is 4.65 eV [20]. The difference in work function (Φ_1- Φ_2) i.e. the flat band potential which is equal to 0.20 eV.

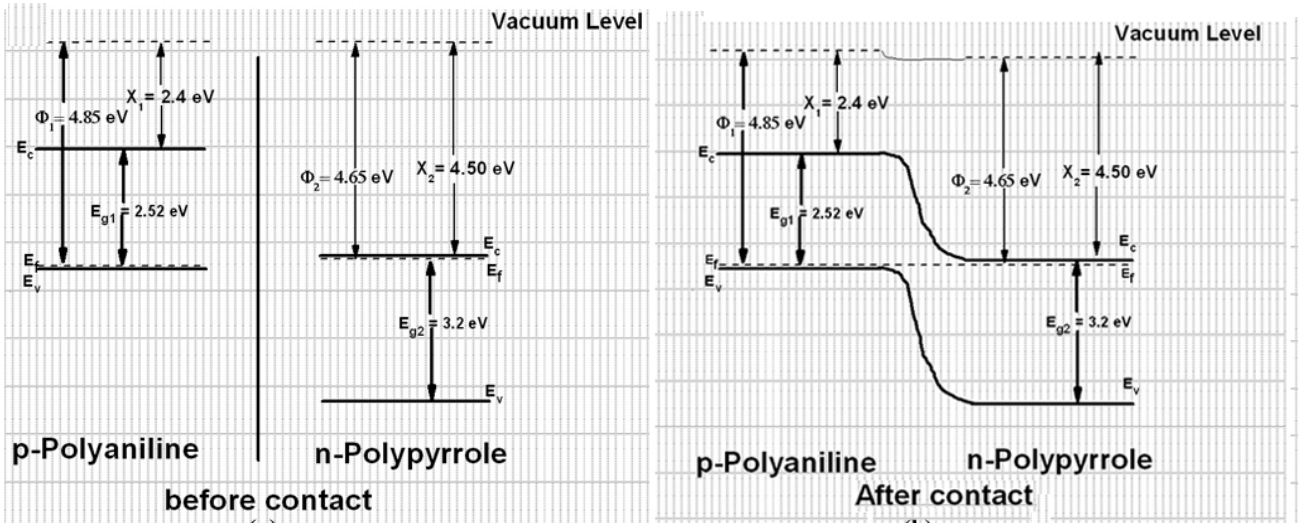

(a) (b)

Fig. 4. Band diagram of n-PPy/p-PANI heterojunction before (a) and after (b) contact.

3. Results and Discussion

3.1. Structural Studies

Fig. 5 shows the XRD patterns of (a) polyaniline and (b) polypyrrole thin films. Polyaniline and polypyrrole thin films are analyzed with Philips X-ray diffractometer (Philips PW 3710) with Cr K_{α} radiation (λ =2.2896 A^0). The absence of sharp peaks indicates that both the electrodeposited polyaniline and polypyrrole thin films are amorphous. Similar types of results are obtained by Dhawale et al [14] for galvanostatically deposited polyaniline thin films and Chougule et al [21] for polypyrrole thin films deposited by chemical oxidative polymerization technique. The peaks observed in XRD patterns are due to the stainless steel substrate and are marked by triangles.

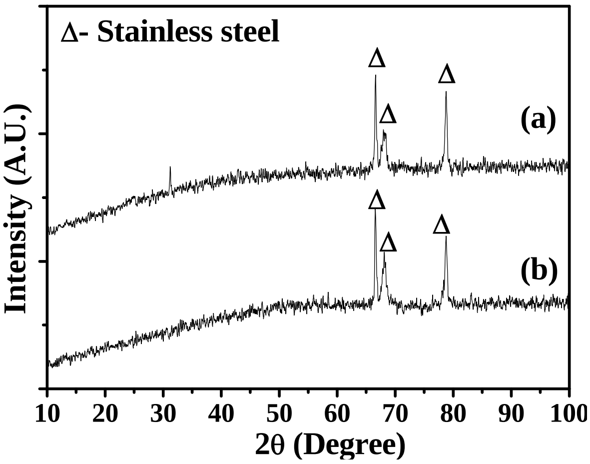

Fig. 5. XRD patterns of (a) polyaniline and (b) polypyrrole thin films on to stainless steel substrate.

3.2. Morphological Studies

The microstructure of polyaniline and polypyrrole thin films is shown in Fig. 6 (a, b). For polyaniline thin films (Fig. 6 (a)), nanofibrous network is observed with many pores. The pore structure plays important role in gas sensing, as the gas species can easily react with film interface. Polypyrrole thin film showed compact nano bundles, which are well adherent to stainless steel substrate (Fig. 6 (b)).

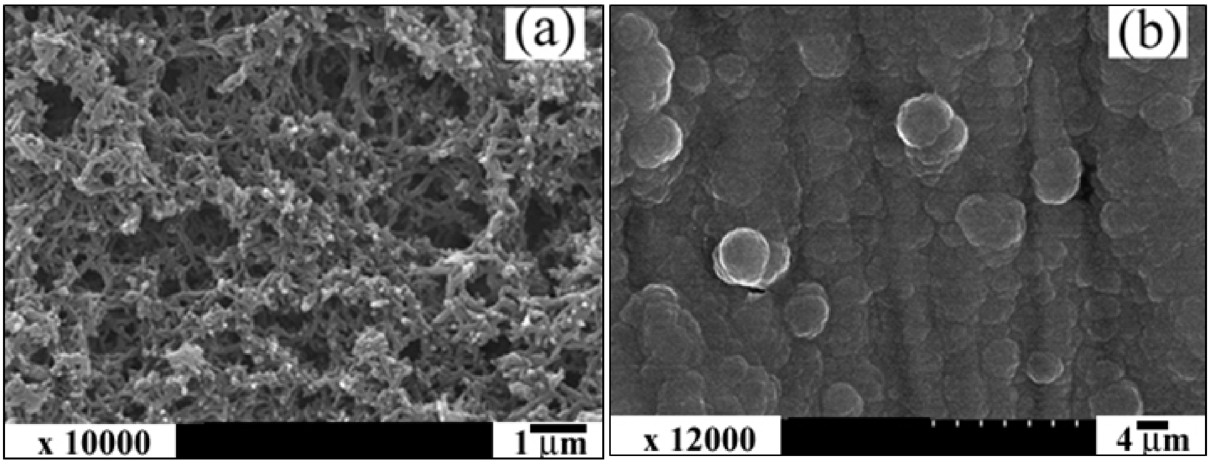

Fig. 6. SEM images of (a) polyaniline, and (b) polypyrrole thin films.

3.3. Raman Study

Fig. 7 shows Raman spectra of polyaniline and polypyrrole thin films. It is well known that vibrational spectrum provides information about chemical structure of polymer. Fig. 7(a) shows Raman spectrum of electrodeposited polyaniline. Different peaks at 1607, 1492, 1339, 1254, 1171 cm^{-1} are observed. The sharp peaks observed at 1607 and 1492 cm^{-1} are assigned to C=C, C-C stretching vibration of quinoid ring and benzonoid ring, respectively as reported by Dhawale et al [22]. Observed peaks which are in the region 1340 and 1260 cm^{-1} are assigned to C-N and $C\text{-}N^+$ stretching vibrations and less intense peak at 1171 cm^{-1} has been assigned to C-H stretching vibration [23]. Fig. 7 (b) shows Raman spectrum of polypyrrole thin film. The initial peak at 930.5 cm^{-1} may be due to the polypyrrole ring deformation [24]. The peak at 1299 cm^{-1} is assigned to the antisymmetrical C–H in-plane bending while other peak at 1382 cm^{-1} is attributed to the ring stretching mode of polypyrrole [25]. The Raman spectra confirmed the formation of polyaniline and polypyrrole.

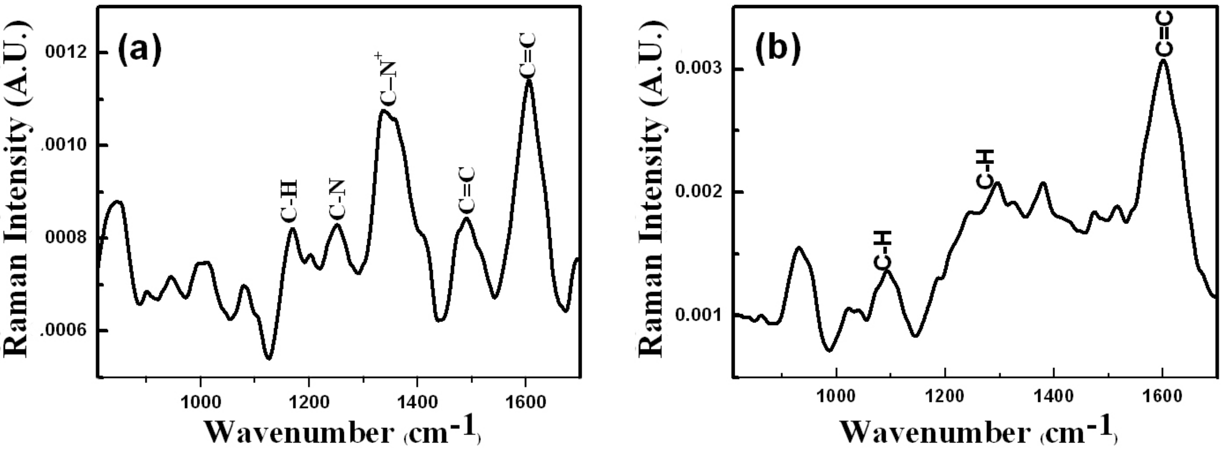

Fig. 7. Raman spectra of (a) PANI, and (b) PPy thin films.

3.4. Selectivity

The ability of a gas sensor to respond to a certain gas in the presence of other gases is known as selectivity or specificity. The forward biased I-V characteristics were recorded of the n-PPy/p-PANI heterojunction films at 1040 ppm concentration of N_2, CO_2 and LPG at room temperature as shown in Fig. 8 (a). Fig. 8 (i) is I-V characteristic before exposure to the gas. Fig. 8(ii) to (iv) are the plots when the heterojunction exposed to different gases at 1040 ppm. The heterojunction offered maximum response towards LPG (33 %) as compared to N_2 (24 %) and CO_2 (17 %) at room temperature. A comparative bar graph of gas response of n-PPy/p-PANI heterojunction thin films to N_2, CO_2 and LPG at room temperature is represented in Fig. 8(b). The heterojunction showed more selectivity for LPG over N_2 and CO_2 at room temperature (300 K). Therefore, further study has been carried out for LPG.

3.5. Gas Sensing Performance of n-PPy/p-PANI Heterojunction

Fig. 9 is forward biased I-V characteristics of n-PPy/p-PANI heterojunction in absence and presence of LPG at room temperature. Through the external connections made to n-PPy/p-PANI heterojunction, the I-V characteristics were recorded in presence of LPG for concentrations ranging from 260 to 1300 ppm. As the heterojunction is exposed to LPG, it shows decrease in current. The decrease in current may be attributed either by change in carrier concentration at heterojunction changing the resistivity of sample or by change in potential barrier at the heterojunction [14]. The heterojunction showed maximum response of 33 % towards LPG for concentration 1040 ppm at room temperature. Dhawale et al. [11, 14] reported 80 % and 63 % gas responses for CdS/polyaniline and TiO_2/polyaniline heterojunctions, respectively. Similarly, Joshi et al. [15, 17] reported maximum gas responses up to 70 % and 67.7 % for CdTe/polyaniline and CdSe/polyaniline heterojunctions, respectively.

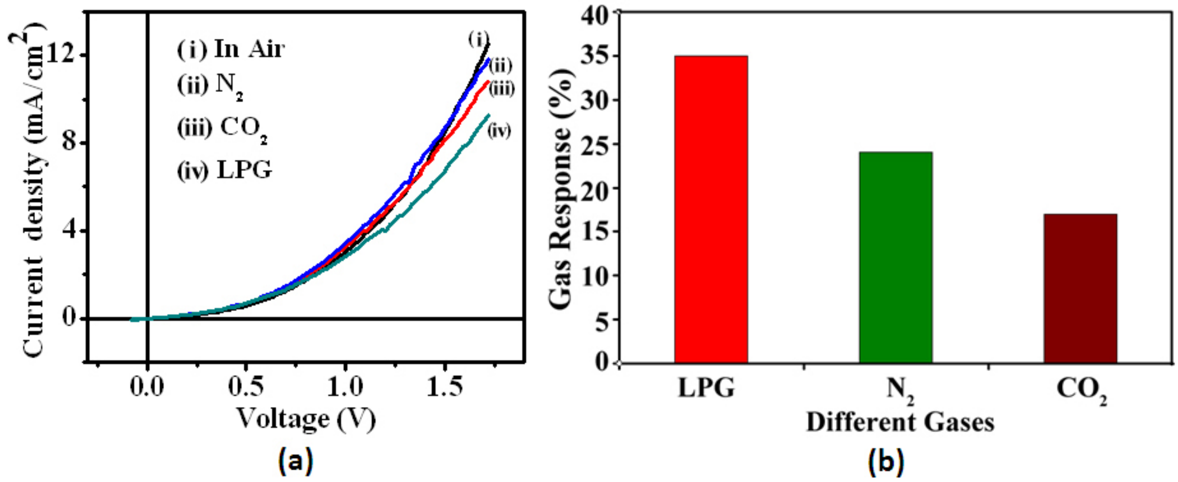

Fig. 8. (a) Forward biased I-V characteristics of p-PANI/n-PPy heterojunction for different gases at fixed concentration of 1040 ppm and (b) Bar graph of gas response to LPG, N_2 and CO_2 and at room temperature.

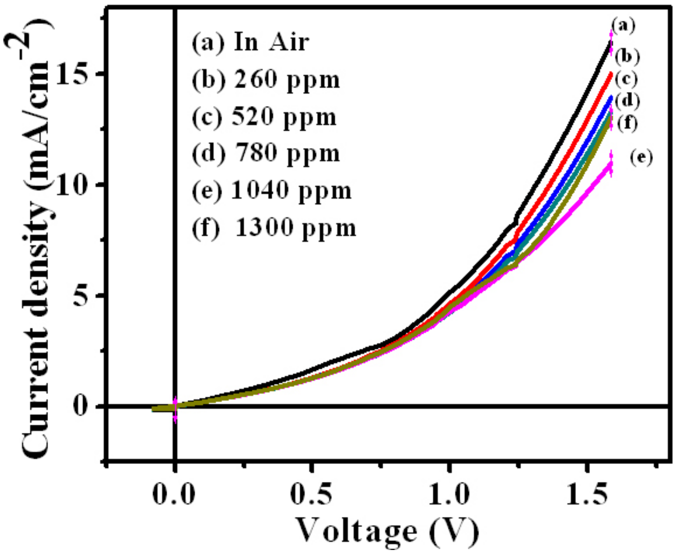

Fig. 9. Forward biased I-V characteristics of n-PPy/p-PANI heterojunction in air and presence of LPG at room temperature.

Fig. 10(a) and (b) shows the schematic representation of n-PPy/p-PANI heterojunction for LPG detection at room temperature and Fig. 10 (a') and (b') shows corresponding model before and after the exposure of LPG respectively. Reducing LPG molecules modulates the carrier concentration near the interface of n-PPy/p-PANI heterojunction upon exposure of LPG which results into increase in potential barrier at the heterojunction interface (Fig. 10(b)'). The barrier height 'Φ_B' increased with increase in LPG gas concentration [14, 16].

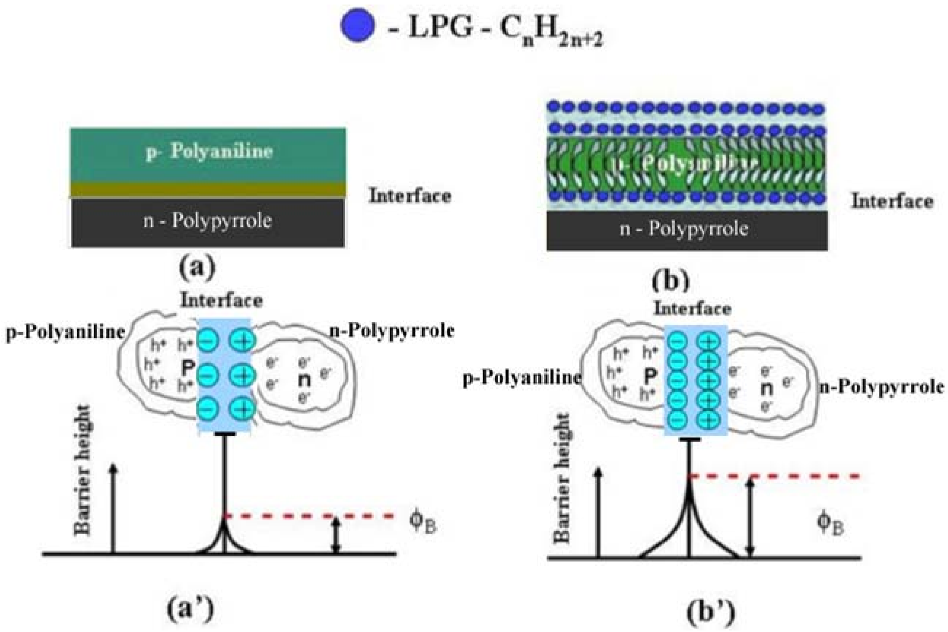

Fig. 10. (a) and (b) schematic representation of n-PPy/p-PANI heterojunction and (a') and (b') the models of heterojunction before and after LPG response.

3.6. Effect of Humidity on Gas Sensing Properties

It is well known that interaction with water vapor increases the conductivity of polyaniline and other conducting polymers [28]. Thus, humidity surrounding a sensor can influence the LPG sensing capability of n-PPy/p-PANI heterojunction. Humidity study was carried out in a humidity chamber. The forward biased current of n-PPy/p-PANI heterojunction was decreased with increase in humidity. The decrease in current may be due to the water vapors which get adsorbed on the thin film interface changing the resistivity of the n-PPy/p-PANI heterojunction [29]. The heterojunction was kept at 60 % humidity for one hour in order to study the humidity duration effect on sensing properties. Fig. 11(I) illustrates the forward biased I-V characteristics of n-PPy/p-PANI heterojunction recorded (a) in air without LPG, (b) in presence of 1040 ppm of LPG before humidity treatment and (c) in presence of 1040 ppm of LPG after one hour humidity treatment at room temperature. The forward biased current density of heterojunction decreased from 14 mA/cm^2 to 6.1 mA/cm^2 at relative humidity 60 %. Hence the sensitivity n-PPy/p-PANI heterojunction decreased from 33 % (± 3 %) to 12 % (± 3 %) upon exposure of LPG. Fig. 11(II) shows the graph of sensitivity of n-PPy/p-PANI heterojunction with gas concentration before and after humidity effect. From the graph, it can be clearly seen that relative humidity affects the gas sensitivity of n-PPy/p-PANI heterojunction. Maximum sensitivity of 33 % (± 3 %) was achieved at 1040 ppm of LPG.

3.7. Response and Recovery Studies

The time required to reach 90% of the final change in current, when the gas is turned on is called as response time and the time taken by sensor to regain original analyte concentration after removal of gas is called as recovery time. Fig. 12 illustrates values of gas response (%) with time of n-PPy/p-PANI heterojunction at a fixed voltage of + 1.6 V for 1040 ppm of LPG. From the plot it is seen that response time of n-PPy/p-PANI heterojunction is 154 s and recovery time is 161 s.

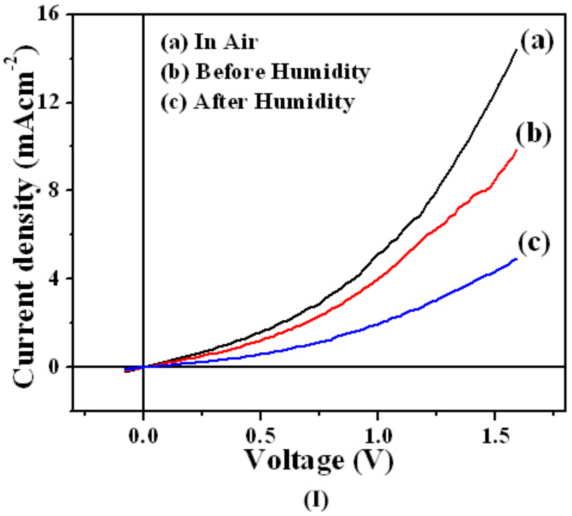

Fig. 11(I). Forward biased I-V characteristics of n-PPy/p-PANI heterojunction (a) in air, (b) before humidity (c) after humidity in presence of 1040 ppm of LPG at room temperature.

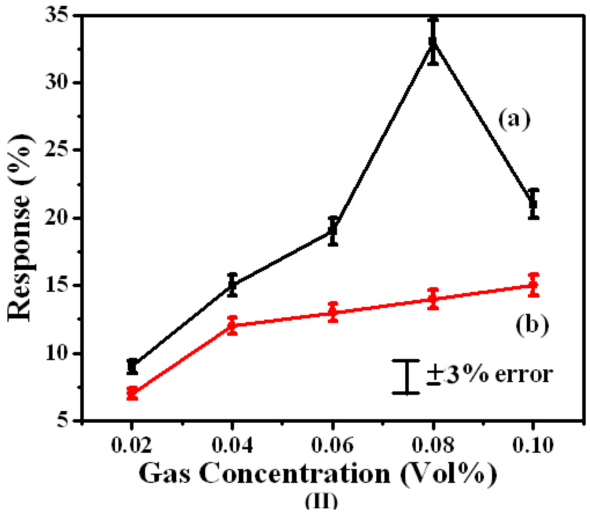

Fig. 11(II). Plot of gas response of n-PPy/p-PANI heterojunction at different LPG concentrations (a) before and (b) after humidity exposure.

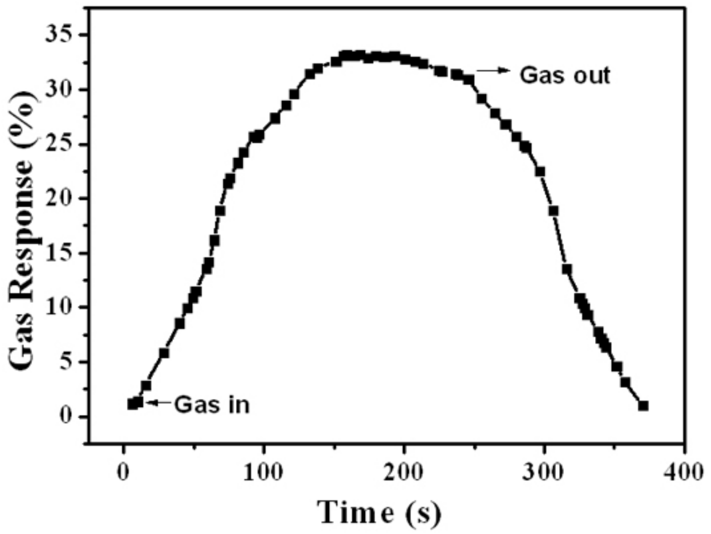

Fig. 12. LPG response (%) vs. time (s) of n-PPy/p-PANI heterojunction at a fixed voltage of + 1.6 V for 1040 ppm of LPG.

4. Conclusions

The n-PPy/p-PANI heterojunction was fabricated using simple electrodeposition method. The presence of characteristic bonds of polyaniline and polypyrrole were confirmed from Raman spectra. The n-PPy/p-PANI heterojunction was found sensitive to LPG as compared to N_2 and CO_2. The n-PPy/p-PANI heterojunction showed 33 % (± 3 %) sensitivity upon exposure of LPG. The relative humidity affects the gas sensing properties of n-PPy/p-PANI heterojunction. The sensitivity decreased from 33 % (± 3 %) to 12 % (± 3 %) upon exposure of 1040 ppm of LPG. The response and recovery times are 154 s and 161 s, respectively.

Acknowledgement

Authors are grateful to the Department of Science and Technology, New Delhi for financial support through the scheme no. SR/S2/CMP-82/2006. S. V. Patil is very thankful to Dr. D. P. Dubal for experimental help and discussions.

References

[1]. Sofian M. Kanan, Oussama M. El-Kadri, Imad A. Abu-Yousef and Marsha C. Kanan, Semiconducting Metal Oxide Based Sensors for Selective Gas Pollutant Detection, *Sensors*, 9, 2009, pp. 8158-8196.

[2]. A. M. More, J. L. Gunjakar, C. D. Lokhande, Liquefied petroleum gas (LPG) sensor properties of interconnected web-like structured sprayed TiO_2 films, *Sens. Actuators B,* 129, 2008, pp. 671-677.

[3]. R. R. Salunkhe, V. R. Shinde, C. D. Lokhande, Liquefied petroleum gas (LPG) sensing properties of nanocrystalline CdO thin films prepared by chemical route: Effect of molarities of precursor solution, *Sens. Actuators B,* 133, 2008, pp. 296-301.

[4]. A. Forta, M. Mugnainia, S. Rocchia, V. Vignolia, E. Cominib, G. Fagliab and A. Ponzonib, Metal-oxide nanowire sensors for CO detection: Characterization and modeling, *Sens. Actuators B,* 148, 2010, pp. 283-291.

[5]. J. L. Gunjakar, A. M. More, C. D. Lokhande, Chemical deposition of nanocrystalline nickel oxide from urea containing bath and its use in liquefied petroleum gas sensor, *Sens. Actuators B*, 131, 2008, pp. 356–361.

[6]. Rajesh, T. Ahuja, D. Kumar, Recent progress in the development of nano-structured conducting polymers/nanocomposites for sensor applications, *Sens. Actuators B: Chem.*, 136, 2009, pp. 275- 286.

[7]. R. Arsat, X. F. Yu, Y. X. Li, W. Wlodarski, K. Kalantar-Zadeh, Hydrogen gas sensor based on highly ordered polyaniline nanofibers, *Sens. Actuators B,* 137, 2009, pp. 529–532.

[8]. M. M. Ayad, N. A. Salahuddin, M. O. Alghaysh, R. M. Issa, Phosphoric acid and pH sensors based on polyaniline films, *Current Applied Physics,* 10, 2010, pp. 235–240.

[9]. S. C. Hernandez, D. Chaudhuri, W. Chen, N. V. Myung, A. Mulchandani, Single Polypyrrole Nanowire Ammonia Gas Sensor, *Electroanalysis*, 19, 2007, pp. 2125- 2130.

[10].Xiaoming Yang, Liang Li, Polypyrrole nanofibers synthesized via reactive template approach and their NH_3 gas sensitivity, *Synthetic Metals*, 160, 2010, pp. 1365–1367.

[11].Kunjal Parikh, Kyle Cattanach, Rashmi Rao, Dong-Seok Suh, Aimei Wu, Sanjeev K. Manohar, Flexible vapour sensors using single walled carbon nanotubes, *Sens. Actuators B,* 113, 2006, pp. 55–63.

[12].Laith Al-Mashat, Henry D. Tran, Wojtek Wlodarski, Richard B. Kaner, Kourosh Kalantar-zadeh, Polypyrrole nanofiber surface acoustic wave gas sensors, *Sens. Actuators B,* 134, 2008, pp. 826–831.

[13].D. S. Dhawale, D. P. Dubal, V. S. Jamadade, R. R. Salunkhe, S. S. Joshi, C. D. Lokhande, Room temperature LPG sensor based on n-CdS/p-polyaniline heterojunction, *Sens. Actuators B,* 145, 2010, pp. 205-210.

[14].J. Herrán, O. Fernández-González, I. Castro-Hurtado, T. Romero, G. Mandayo, E. Castano, Photoactivated solid-state gas sensor for carbon dioxide detection at room temperature, *Sens. Actuators B*, 149, 2010, pp. 368–372.

[15].R D. Ladhe, P. K. Baviskar, W. W. Tan, J. B. Zhang, C. D. Lokhande and B. R. Sankapal, LPG sensor based on complete inorganic n-Bi_2S_3-p-CuSCN heterojunction synthesized by a simple chemical route, *J. Phys. D: Appl. Phys.,* 43, 2010, p. 245302.

[16].D. S. Dhawale, R. R. Salunkhe, U. M. Patil, K. V. Gurav, A. M. More, C. D. Lokhande, Room temperature liquefied petroleum gas (LPG) sensor based on p-polyaniline/n-TiO_2 heterojunction, *Sens. and Actuators B*, 134, 2008, pp. 988–992.

[17].S. S. Joshi, T. P. Gujar, V. R. Shinde and C. D. Lokhande, Fabrication of n-CdTe/p-polyaniline heterojunction based room temperature LPG sensor, *Sens. and Actuators B*, 132, 2008, pp. 349–355.

[18].D. S. Dhawale, D. P. Dubal, A. M. More, T. P. Gujar and C. D. Lokhande, Room temperature liquefied petroleum gas (LPG) sensor, *Sens. and Actuators B*, 147, 2010, pp. 488-494.

[19].S. S. Joshi, C. D. Lokhande, Sung-Hwan Han, A room temperature liquefied petroleum gas sensor based on all-electrodeposited n-CdSe/p-polyaniline junction, *Sens. and Actuators B*, 123, 2007, pp. 240–245.

[20].Alain Deronzier, Jean-Claude Moutet, Polypyrrole films containing metal complexes: syntheses and applications, *Coordination Chemistry Reviews,* 147, 1996, pp. 339-371.

[21].S. S. Joshi, C. D. Lokhande, Fabrication of isotype (p-p) selenium–polyaniline heterojunction diode by electrochemical method, *Applied Surface Science,* 252, 2006, pp. 8539–8543.
[22].D. Tsamouras, E. Dalas, S. Sakkopoulos and E. Vitoratos, Characterization of sulfide/ polyaniline and sulfide/ polypyrrole contacts, *Appl. Surf. Sci.,* 65/66, 1993, pp. 388-393.
[23].Manik A. Chougule, Shailesh G. Pawar, Prasad R. Godse, Ramesh N. Mulik, Shashwati Sen, Vikas B. Patil, Synthesis and Characterization of Polypyrrole (PPy) Thin Films, *Soft Nanoscience Letters,* 1, 2011, pp. 6-10.
[24].D. S. Dhawale, R. R. Salunkhe, V. S. Jamadade, T. P. Gujar and C. D. Lokhande, An approach towards the growth of polyaniline nanograins by electrochemical route, *Applied Surface Science,* 255, 2009, pp. 8213-8216.
[25].R. Mažeikienė, V. Tomkutė, Z. Kuodis, G. Niaura, A. Malinauskas, Raman spectro electrochemical study of polyaniline and sulfonated polyaniline in solutions of different pH, *Vib. Spectrosc.,* 44, 2007, pp. 201-208.
[26].Yueping Fang, Jianwei Liu, Deok Jin Yu, James P. Wicksted, Kaan Kalkan, C. Ozge Topal, Bret N. Flanders, JudyWu, Jun Li, Self-supported supercapacitor membranes: Polypyrrole-coated carbon nanotube networks enabled by pulsed electrodeposition, *J. Power Sources,* 195, 2010, pp. 674–679.
[27].Y. F. Chen, J. Liu, H. J. Yao, D. Mo, J. L. Duan, M. D. Hou, Y. M. Sun, L. Zhang, K. Maaz, Electrochemical polymerization and characterization of polypyrrole nanowires and nanotubules, *Physica B*, 405, 2010, pp. 2461–2465.
[28].M. Angelopoulos, A. Ray, A. G. MacDiarmid, A. J. Epstein, Polyaniline: processability from aqueous solutions and effect of water vapor on conductivity, *Synth. Met.*, 21, 1987, pp. 21–30.
[29].M. Matsuguchi, A. Okamoto, Y. Sakai, Effect of humidity on NH_3 gas sensitivity of polyaniline blend films, *Sens. and Actuators B,* 94, 2003, pp. 46–52.
[30].T. A. Skotheim, Handbook of conducting polymers, *Marcel Dekker,* New York, 1986, pp. 1369-1375.
